ORIGINAL PAPER

Check for
updates

Drug-loaded PCL electrospun nanofibers as anti-pancreatic cancer drug delivery systems

Oihane Mitxelena-Iribarren[1,2] · Marc Riera-Pons[1,2] · Sheila Pereira[3,4] ·
Francisco José Calero-Castro[3,4] · Juan Manuel Castillo Tuñón[5] ·
Javier Padillo-Ruiz[3,4,6] · Maite Mujika[1,2] · Sergio Arana[1,2]

© The Author(s) 2022

Abstract

Cancer is one of the main causes of death worldwide, being pancreatic cancer the second deadliest cancer in Western countries. Surgery, chemotherapy and radiotherapy form the basis of pancreatic cancer's current treatment. However, these techniques have several disadvantages, such as surgery complications, chemotherapy systemic side effects and cancer recurrence. Drug delivery systems can reduce side effects, increasing the effectivity of the treatment by a controlled release at the targeted tumor cells. In this context, coaxial electrospun fibers can increase the control on the release profile of the drug. The aim of this study was to encapsulate and release different anticancer drugs (5-Fluorouracil and Methotrexate) from a polymeric fiber mat. Different flows and ratios were used to test their effect on fiber morphology, FTIR spectrum, drug encapsulation and release. Good integration of the anticancer drugs was observed and the use of a desiccator for 24 h showed to be a key step to remove solvent remanence. Moreover, the results of this study demonstrated that the polymeric solution could be used to encapsulate and release different drugs to treat cancers. This makes coaxial electrospinning a promising alternative to deliver complex chemotherapies that involve more than one drug, such as FOLFIRINOX, used in pancreatic cancer treatment.

Keywords Drug delivery · Electrospinning · Anticancer · 5-fluorouracil · Methotrexate

Introduction

Cancer is one of the deadliest diseases worldwide. One of the worst prognoses of this disease is for the pancreatic cancer, as only the 4% of the patients survive after 5 years of the diagnosis date[1, 2]. It is also the second most deadly cancer-related cause in Western countries[3]. Surgery, chemotherapy such as FOLFIRINOX or Gemcitabine, and radiotherapy are the most common treatments used to treat this illness [1, 4–6]. However, they have strong disadvantages such as chemotherapy systemic side effects, limitations of techniques and recurrence due to rests of cancer not removed during the treatment, among others [7, 8]

These disadvantages and limitations can be reduced if drug delivery systems (DDSs) are used during the healing process[9]. The main advantage of these technologies is a focalized and more efficient delivery, which derives on a reduction in the side effects and tumor recurrence[10]. Polymers are the main vehicles used for DDS because of the wide range of macromolecules that can be used. Each of them has a specific biodegradation profile[11], which can provide a controlled delivery as the degradation kinetics will describe the drug release profile[12]. For example, polycaprolactone (PCL) is a biodegradable polymer widely used as DDS, even with encapsulated anticancer drugs [13–16].

DDS can be divided into two groups, depending on the liberation profile they have: they can do it systematically (such as the case of nanoparticles) or locally (as in the case of electrospun fibers, films or hydrogels)[17]. Systemic delivery systems can be injected or introduced orally[18]. The main advantages of these systems are their nanometric size, specificity and low invasiveness, as the vehicles can reach smaller vessels and can be engineered to recognize certain receptors and no surgery is required for the treatment [19–21]. On the other hand, sometimes these particles are hard to functionalize or can lose their specificity due to the lack of molecules that can identify the target and the interactions in the delivery process[22].

Local drug delivery systems release the drug in a specific site, loco-regionally, by diffusion or degradation mainly[23]. These systems can take several forms, such as foams, hydrogels or fibers among others[10, 24, 25]. This technology has a strong background, as it has been in the market since 1995 when GLIADEL® wafers were commercialized to treat brain cancers. The main disadvantage of hydrogels or foams is that the drug is delivered by diffusion[10], which is a fast occurring phenomenon that releases the drug in a short period of time[26]. Even more, the target of local DDS is not accessible without surgery. That is why these devices are meant to be complementary to conventional surgery, in order to ensure that the entire tumor is removed.

Electrospinning is a fabrication process to obtain a local DDS. This method is easy to use and versatile, it generates high surface-to-volume ratio meshes, and it usually is a low-cost process[27]. The generated scaffolds are formed by fibers, which have a mixed delivery profile, as both diffusion and degradation related release occur[19, 25]. The shape and size of the fibers play an important role in the drug releasing profile. Therefore, there are several parameters that can be

altered to modify the size of those electrospun fibers in order to control the drug release, such as potential difference, nozzle–collector distance, polymeric solution flow, polymer concentration and conductivity[28–31]. One limitation of this technique is that the fiber has the same properties across its whole structure and a burst drug release can occur, as the molecule is totally blended with the fiber[16]. This can be solved if two solutions are injected at the same time by coaxial electrospinning, increasing the versatility and the control on the coaxial fiber properties, composition and drug loading and release[32, 33]. Briefly, coaxial electrospinning is a modification of the conventional electrospinning process, where more than one solution is electrospun [34]. The spinnerets containing the different solutions share an axis. This allows the injection of one solution into the other at the needle tip: the core fluid is drawn within the outer one to produce continuous filled nanofibers.

Actual chemotherapy treatments use various drugs, such as 5-Fluorouracil (5F), irinotecan, oxaliplatin and folinic acid at the same time to treat pancreatic cancer cells[35–37]. In addition, including other drugs such as painkillers in the treatment could improve the patient's life quality. Therefore, testing PCL to encapsulate drugs related to general cancer treatment, such as Methotrexate (MTX), is a required step to keep DDS on the same road that chemotherapy is undergoing. For this reason, in order to obtain an alternative treatment for pancreatic cancer, PCL was used to encapsulate and release different antineoplastic molecules by coaxial electrospinning. PCL-blended nanofibers loaded either with 5F or MTX were investigated in this research. Various PCL proportions and fabrication parameters were used to produce different electrospun nanofibers. The effect of those specifications in nanofiber characteristics and drug release was studied in this work.

Methods

Materials

Polycaprolactone (PCL, Mw = 100 000 g/mol), 99% chloroform, 100% methanol, 98–100% formic acid and 99% acetic acid were purchased from Sigma Life Sciences, USA. 5-Fluorouracil (5F) was purchased from AK Scientific Inc, USA, and Methotrexate (MTX) was kindly provided by Dr. A. Aldaz, from the Department of Pharmacy of Clínica Universidad de Navarra, Spain.

Electrospinning of PCL nanofibers

Electrospinning solutions were prepared by dissolving 14 wt.% of PCL in formic acid/acetic acid/chloroform with a ratio of 47.5: 47.5: 5 (v/v/v), respectively. The solution was stirred at room temperature overnight and used within the first 72 h. A second solution was prepared for each drug, 5F and MTX, by adding 28 mg/mL or 8.4 mg/mL, respectively, to the original polymeric solution.

Fig. 1 **a**) Coaxial electrospinning set-up; **b**) coaxial nozzle of Ramé-Hart Instrument Co; **c**) schematic of the coaxial electrospinning process

Once the solutions were ready, coaxial electrospinning was used to electrospun the nanofibers (Fig. 1a). The setup consisted of a coaxial nozzle with an inner gauge of 26G and an outer gauge of 18G (Ramé-Hart Instrument Co, USA; Fig. 1b), two syringe pumps (KD Scientific Inc, USA) and a high-voltage DC power supply (Heinzinger, Germany). A schematic of the coaxial electrospinning is shown in Fig. 1c

Three different configurations were used to fabricate the fibers. The parameters used for each configuration tested are shown in Table 1. These parameters were based on the study of Iqbal et al. (2017). The scaffolds fabricated only with the polymeric solution were used as control and identified with the code CoPP. The drug-loaded fibers were fabricated using either of the drug-solutions in the inner tube and the polymeric solution in the outer one. The fibers loaded with 5F were identified as P5F and the ones loaded with MTX as PMTX.

Characterization of nanofibers

Surface morphology

To assess the morphology of the nanofibers, scanning electron microscopy (SEM, Phenom G2 Pro, USA) was used. The diameter of the fibers was measured by using ImageJ software (National Institute of Health). A total of 4 images per scaffold were analyzed by measuring the diameter of 25 fibers per frame. Therefore, the diameter of 100 fibers was measured randomly in each sample and the average diameter

Table 1 Electrospinning fabrication parameters of the three different configurations, with and without drug

Sample code	Collector-nozzle distance (cm)	Power supply (kV)	Outer flow (mL/h)	Inner flow (mL/h)
CoPP1/P5F1/PMTX1	13.5	21	0.20	0.05
CoPP2/P5F2/PMTX2	13.5	21	0.15	0.05
CoPP3/P5F3/PMTX3	13.5	21	0.10	0.05

was reported. Nanofiber mats porosity and pore size were measured also by image analysis, using Diameter J, an ImageJ package. The obtained values are expressed as mean value $\pm$ standard deviation.

Solvent remanence

Fourier transform infrared spectroscopy (FTIR) was undertaken on pure PCL pellets and the three solvents (formic acid, acetic acid and chloroform), as well as on all the electrospun mat samples by the FTIR Spectrum 100 with the ATR (PerkinElmer, USA). The scanning range tested goes from 650 to 4000 cm^{-1} with a total amount of 8 accumulations. In order to perform the FTIR analysis, solid samples were compressed whereas liquid samples were not. Mat samples were analyzed just after being fabricated or after 24 h. In the case of the latter, the electrospun mats were either stored overnight at room temperature or desiccated in a desiccator for the 24 h.

Drug loading efficiency

Differential Scanning Calorimetry (DSC)

Differential scanning calorimetry was used to evaluate the drug integration inside the fibers (DSC, 4000 PerkinElmer). Samples with a mass between 5 and 20 mg were used for the analyses. PCL pellets were used without any further modification, whereas scaffold pieces were cut and weighted in order to normalize the results. The analyzed temperature ranged from 20 to 100 °C, with a temperature increase of 10 °C/min.

FTIR analysis

Drug loading was semiquantitatively assessed by FTIR analysis of the drug-loaded scaffolds. A compressed sample of each drug-loaded mat was analyzed once the solvent was fully evaporated from the fibers. The same equipment, range, and number of accumulations as in solvent perdurability characterization were used in these analyses.

In vitro drug release

The drug release of the different mat types was determined by immersing the loaded nanofibers in PBS. The procedure was as follows: three samples from each configuration for both 5F and MTX mats were cut into 2.25 cm^2 squares and submerged for 2 h in MiliQ water, in order to remove the materials that could be outside the fibers. The mats were then dried and weighted, before being introduced in 15 mL of PBS (pH = 7.4) for two weeks at 37 °C on an orbital shaker (Polymax 1040 from Heidolph, Germany). During this period, spectrophotometry was used to characterize drug release: 100 μl of the immersing PBS were taken for absorbance reading every

24 h. In order to determine the released drug amount, the respective calibration curve was obtained for each drug. Beer-Lambert equations were used to calculate drug concentration at $\lambda = 270$ nm and $\lambda = 350$ nm for 5F and MTX respectively. The fitted line for calibration of 5F in PBS is according to Eq. 1 and the amount of R^2 is 0.9411. On the other hand, MTX calibration followed Eq. 2, with a R^2 of 0.9164.

$$Y = 3.5564x^{0.0086} \tag{1}$$

$$Y = 6.9286x + 3.8287 \tag{2}$$

Statistical analysis

To end up with the statistical analysis, independent Student's t test was performed to compare the effect of drugs and different electrospinning configurations on fiber diameter.

The statistical significance criterion was the same for all the analyses. Statistical difference was determined as not significant (p-value > 0.05), significant ($0.01 < p$-value < 0.05), very significant ($0.001 < p$-value < 0.01) or extremely significant (p-value < 0.001).

RESULTS AND DISCUSSION

Surface morphology

SEM was used to observe the nanofibers morphology and diameter for the different configurations tested with and without the drugs. The images obtained by SEM (Fig. 2) showed that all configurations produced nanofibers, which had a great surface to volume ratio. No drug crystals or other deformations such as beads were observed in any of the images obtained, as all polymeric mats presented homogeneous fibers of different diameters. All fibers were in the nanofiber range as the maximum average diameters were less than 400 microns. The mats with greater diameters were the ones without drug encapsulation (Table 2), as all three samples had thicker fibers than any of the mats blended with drug. These differences were probably caused due to the conductivity differences between PCL and the drugs[38]. In addition, the fiber distributions for the scaffolds were overall a Gaussian distribution positively skewed. However, the histograms of the configurations CoPP2 and PMTX1 looked like an inverse ramped distribution rather than a Gaussian.

Significant differences were observed in the fiber diameter when outer flow was decreased from 0.20 mL/h to 0.15 mL/h in the case of control scaffolds, as CoPP1 mats vs CoPP2 ones showed a p-value $= 2.40 \times 10^{-20}$. In addition, reducing the outer flow from 0.15 to 0.10 mL/h, significantly reduced the fiber diameter, between CoPP2 and CoPP3 (p-value $= 8.07 \times 10^{-14}$). When the polymeric solutions were blended with 5F, no significant differences were observed if the outer flow was reduced from 0.20 to 0.15 mL/h nor from 0.15 to 0.10 mL/h. On the other hand, introducing 5F into the mats significantly reduced the fiber diameter with respect
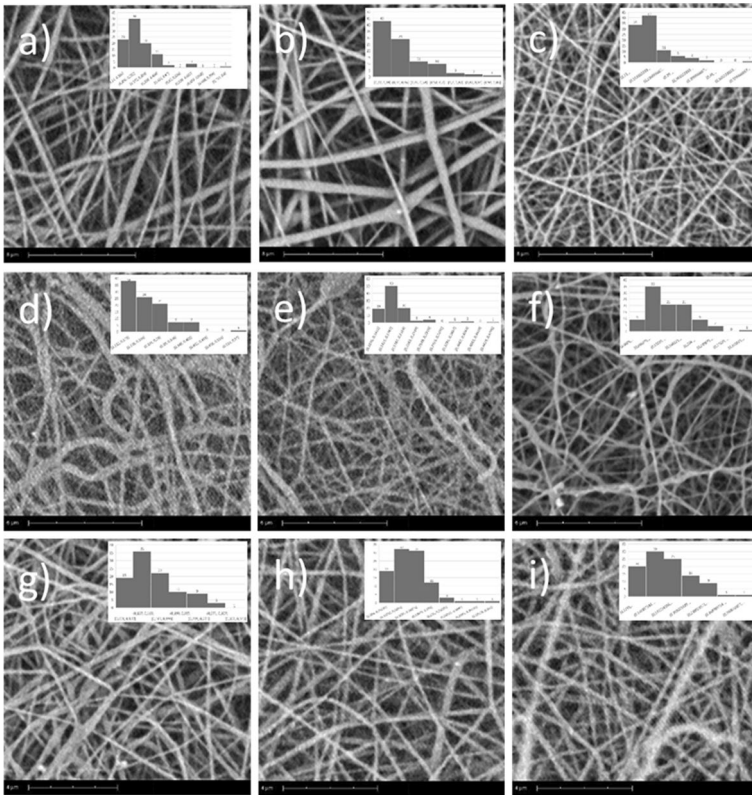
Fig. 2 SEM images with their corresponding histogram of the different electrospun configurations: **a** CoPP1; **b** CoPP2; **c** CoPP3; **d** PMTX1; **e** PMTX2; **f** PMTX3; **g** P5F1; **h** P5F2; **i** P5F3

Table 2 Results of SEM images analysis on morphology (U = uniform, B = beaded), fiber diameter and porosity, according to configuration and blended drug

Code	Morphology			Diameter (μm)			Porosity (%)		
	Control	5F	MTX	Control	5F	MTX	Control	5F	MTX
1	U	U	U	0.26 ± 0.11	0.16 ± 0.06	0.20 ± 0.09	68.87	63.18	50.75
2	U	U	U	0.37 ± 0.18	0.16 ± 0.05	0.17 ± 0.06	56.25	50.27	60.24
3	U	U	U	0.20 ± 0.08	0.17 ± 0.04	0.15 ± 0.05	75.33	64.10	56.52

to the control scaffolds: when the homologous samples were compared, extremely significant difference was observed in the three cases with p-values of 6.84×10^{-13}, 4.76×10^{-20} and 4.17×10^{-4} for CoPP1 versus P5F1, CoPP2 versus P5F2 and CoPP3 versus P5F3, respectively. Similar behaviors were observed in the case of the MTX scaffolds, as all the MTX-blended fibers had extremely significant smaller diameter than the pure polymeric ones (p-vales < 0.001). Moreover, as for the control
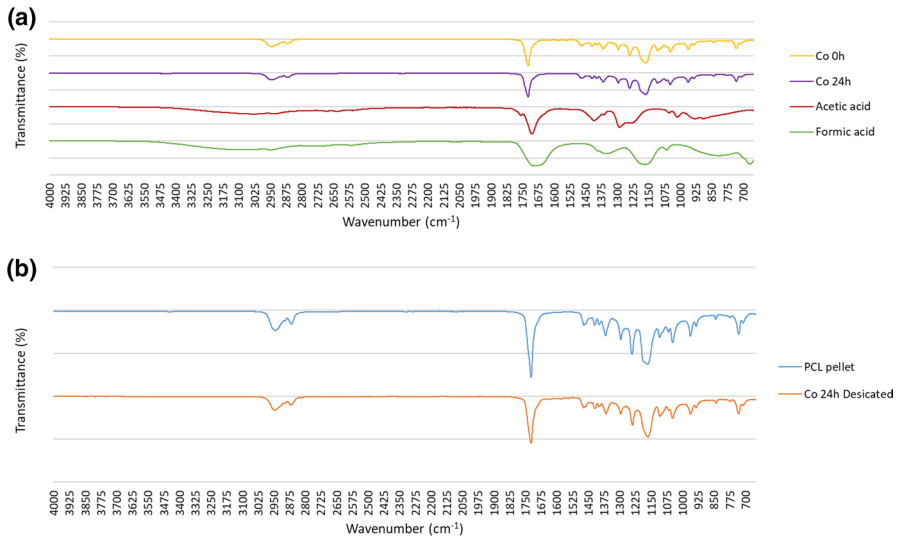
Fig. 3 FTIR spectrum of: **a)** coaxial polymeric mats without drug analyzed right after being electrospun (Co 0 h) or let at room conditions for 24 h before performing the FTIR (Co 24 h), acetic acid and formic acid; **b**) the PCL pellet and a coaxial polymeric mat desiccated for 24 h (Co 24 h Desicated)

polymeric scaffolds, a relationship between the total flow rate and the fiber diameter was observed in MTX-loaded scaffolds. In this case, reducing the outer flow from 0.20 to 0.10 mL/h significantly reduced the fiber diameter (p-value $= 1.27 \times 10^{-6}$). This effect, which was not observed only in the case of 5F, could be due to solution conductivity. MTX is less polar than 5F [39, 40]. Therefore, it was more likely to behave as PCL, ending up in a fiber decreasing effect of the polymeric flow.

Porosity was also evaluated, obtaining porosities in the range of 50–75%. The drug loaded mats had overall less porous scaffolds, as two of the highest porosities obtained belonged to the control group (Table 2). This together with the surface-to-volume ratio improved the drug exposition and enhanced the interaction with the environment by an easy fluid flow through the scaffold. These results together with the fiber uniformity observed in this research matched with the results that Iqbal et al. [16] obtained in their study.

Solvent remanence

The non-desiccated mats did not show exactly the same spectrum as the pellet, as they showed two peaks at 1509 and 1545 cm^{-1}, which correspond to the carboxyl group of the acids present in the solvents (Fig. 3a). This meant that the solvent was not completely removed during the fabrication. Therefore, introducing the scaffold into a body right after being electrospun could cause several problems, as the solvents were not fully evaporated.

Increasing the waiting time to 24 h reduced notoriously the solvent presence, as the depth of the peak was more pronounced in the mat analyzed just after the electrospinning process than in the mat let 24 h under room conditions before performing the FTIR. Nevertheless, the solvent-related peaks were still noticeable.

However, the solvent presence was completely erased after the mat was desiccated for 24 h, as the curve overlapped exactly the same peaks of the curve of the pure polymer pellet (Fig. 3b). This is possible because of the low-pressure environment generated in the desiccator. Therefore, it was proven that this widely used method was completely necessary to get rid of the solvents used in the electrospinning process[16, 41, 42].

Drug loading

The differential scanning calorimetry performed on PCL showed the melting transition of the polymer. No major differences were observed between a PCL mat against a pellet (Fig. 4a), as both samples underwent a solid to liquid transition around 65 °C. The only observable difference was the melting temperature and the heat flow, as the melting temperature was greater for the pellet than the mat: 66.1 °C and 63.7 °C, respectively. The heat flow for the pellet was overall higher. These values concur with the ones observed in the literature[43–45].

On the other hand, both pure MTX and 5F did not show any transition in the analyzed range (Fig. 4b and c), as the curves were completely flat. The scaffolds blended with these molecules showed a peak that was not present in the DSC performed on PCL, around 5 °C. This peak was more notable in the mats blended with MTX. The observed melting point for the mats blended with MTX and 5F was between 62.9–66.0 °C and 62.4–64.1, respectively. The observed difference between the control and the loaded scaffolds could suggest the presence of the drug in the mats.

In addition to the DSC analyses, to further confirm the presence, the infrared spectrum was used to observe the drug loading of MTX and 5F in the fibers (Fig. 5), as shown in the literature[12]. According to these FTIR results, it was concluded that a higher ratio of inner/outer flow in both MTX and 5F-loaded scaffolds was related to a greater drug concentration. As the outer solution did not contain the anticancer drug, a reduction of the outer flow related to the total solution flow induced a greater drug flow, which meant a higher drug encapsulation. This trend was clearer in the fibers blended with 5F at 1661 cm^{-1} and between 3000 and 3300 cm^{-1}, belonging that peak to the C=O stretching and the band to the N–H stretching, respectively. In the case of MTX-loaded scaffolds, the two ranges in which this drug presence was observable were from 1525 to 1617 cm^{-1} and from 3000 to 3500 cm^{-1}, also due to the C=O stretching and the N–H stretching.

Considering that no drug crystals nor deformations on the fibers were observed in the SEM images, and the drug presence observed with both the DSC and FTIR analyses, it was depicted that the drug was successfully encapsulated during the coaxial electrospinning process performed in this study.

(a)

(b)

(c)
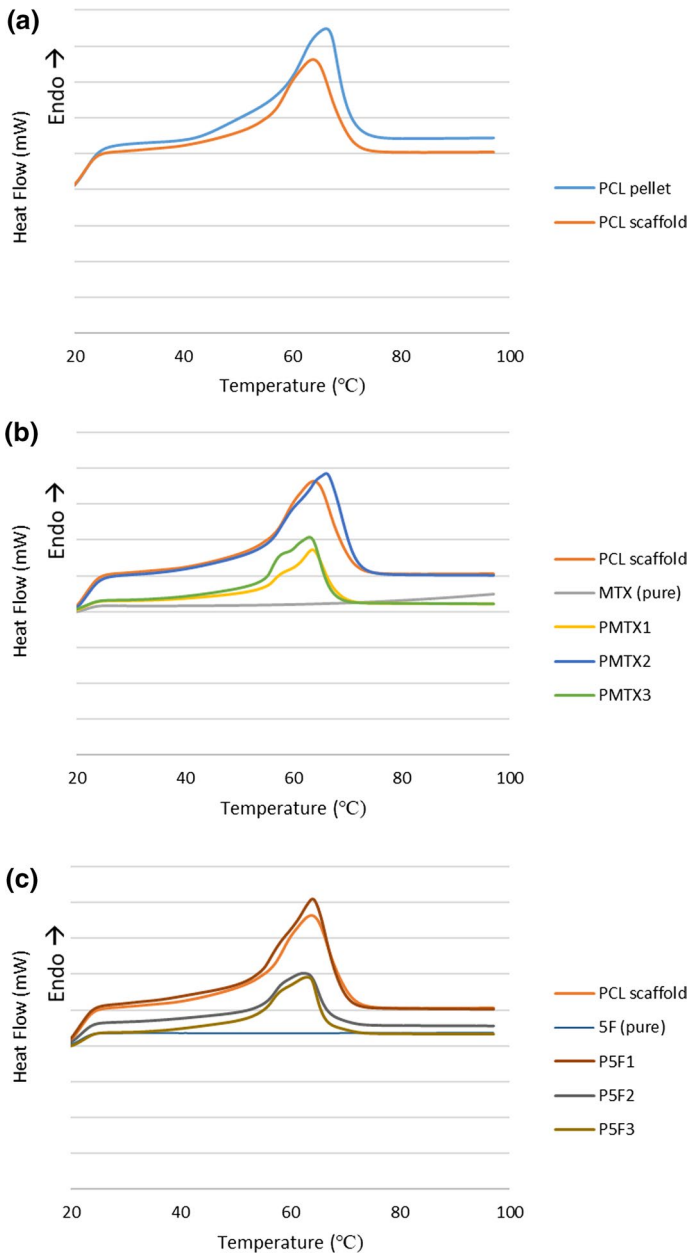
Fig. 4 Differential scanning calorimetry scans of: **a** PCL pellets and a PCL scaffolds; **b** drugless PCL scaffolds, pure MTX and MTX-loaded mats; **c** drugless PCL mats, pure 5F and 5F-blended scaffolds

(a)

(b)

Fig. 5 Comparison of the FTIR spectrum of the PCL pellet and the pure drug with the drug-loaded scaffolds: **a** PCL pellet and pure MTX; **b** MTX-loaded scaffolds; **c** PCL pellet and pure 5F and **d** 5F-loaded scaffolds

(a)

(b)
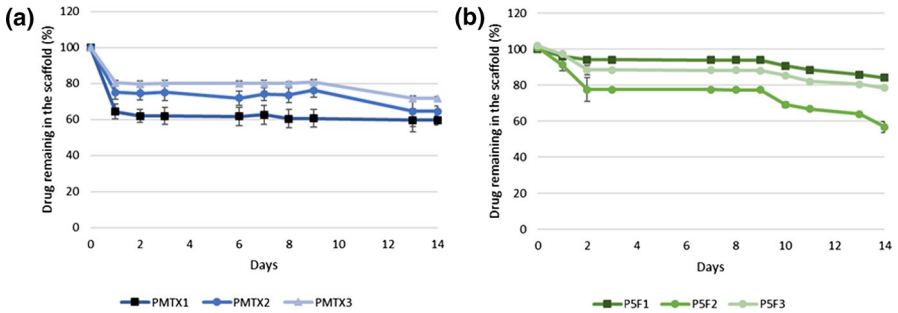
Fig. 6 Drug release profile according to the theoretical mat drug load of **a** MTX-loaded scaffolds and **b** 5F-loaded scaffolds

Drug release

The release profile for MTX suggested that it was mostly released during the first 24 h, as the released percentage did not increase much since the first day (Fig. 6a). In fact, it showed a sustained drug concentration level from the first day until the 9th day. This rapid release was due to drug diffusion rather than due to polymer degradation, because the first one is usually a dominant event in the early stages, while the latter is dominant in long-term release. The release behavior reported in this research was previously observed in several studies[12, 16, 46]. In addition, the percentage of the released drug was greater for all the mats with higher external flows.

On the other hand, 5F mats have shown a different release profile (Fig. 6b), a much lower drug release percentage and a higher relative deviation. The scaffolds containing 5F showed a peak on day 2, similar to the release observed in previous studies[16]. However, afterwards, no drug presence was detected until day 9, which increased slightly during the last five incubation days. The decrease phenomenon observed in the drug release from day 3 could be due to the solubility of 5F, which sometimes precipitate, leading to a non-representative sample of the real release. The P5F2 configuration sample showed a greater release than P5F1 and P5F3. These two demonstrated a similar release profile past the 3rd day of incubation.

The measurement of both MTX and 5F release demonstrated that the coaxial electrospinning process performed in this study generated fibrous scaffolds that could work as a DDS for pancreatic cancer treatment.

Conclusion

In this study, PCL-blended nanofibers containing either MTX or 5F with various electrospinning fabrication parameters were investigated. The anticancer drug-loaded scaffolds were successfully fabricated using the coaxial electrospinning method. The surface morphology of nanofibers analyzed by scanning electron microscopy showed that all the tested configurations produced nanofibers, which had a great surface-to-volume ratio and had no drug crystals remaining on the surface or deformations in the fibers. The addition of the drug into the inner solution led nanofiber diameter to decrease. Although the solvents used in the fabrication method were not fully removed during the electrospinning process, using a desiccator for 24 h after the scaffold was electrospun erased the presence of those solvents. Therefore, this procedure constitutes an essential step to be done before putting the scaffolds in contact with any living organism. Both the drug loading efficiency and the drug released were demonstrated in vitro, making these scaffolds a promising drug delivery system. Both DSC and FTIR analyses confirmed the presence of MTX and 5F, apart from the main polymer PCL, in the electrospun nanofibers. Finally, spectrophotometry was used to quantify drug release, showing a rapid release in the case of MTX from the fibers and a low percentage of release for the 5F-loaded samples. It was observed that drug release in these nanofibers occurred by diffusion or permeation through nanofiber mat matrices, because of very slow degradation of nanofiber mats was observed during the release period.

Even though further studies must be done to test the cytotoxicity and effectivity of the scaffold in vivo, it was concluded that the production of electrospun nanofibers is a promising method to encapsulate and release anticancer drugs such as 5-Fluorouracil and Methotrexate. The fibers fabricated in this study had a high surface-to-volume ratio, which would increase the interaction between the mesh and its environment once inserted in the body. Moreover, the versatility of the coaxial electrospinning process performed in this study is a great advantage among another DDS. In these systems, the amount of drug to deliver can be controlled according to the requirements of the patient changing the fabrication parameters, giving a greater control on fiber properties and therefore drug release. The reduction of side

effects due to a localized release is also a massive advantage to use electrospinning to encapsulate anticancer drugs.

Data availability The datasets generated during and/or analyzed during the current study are available from the corresponding author on reasonable request.

Declarations

Conflict of interest The authors have no relevant financial or non-financial interests to disclose.

Consent for publication No human subjects participated in this study. (Not applicable).

Ethical approval.
No human being participated in this study. No animal was used in this study. The experiments comply with the current laws of the country in which they were performed.

References

1. Kamisawa T, Wood LD, Itoi T, Takaori K (2016) Pancreatic cancer. Lancet 388:73–85
2. Seoane-Mato D, Nuñez O, Fernández-de-Larrea N et al (2018) Long-term trends in pancreatic cancer mortality in Spain (1952–2012). BMC Cancer 18:1–10. https://doi.org/10.1186/s12885-018-4494-3
3. Rahib L, Smith BD, Aizenberg R et al (2014) Projecting cancer incidence and deaths to 2030: The unexpected burden of thyroid, liver, and pancreas cancers in the united states. Cancer Res 74:2913–2921
4. Beger HG, Rau B, Gansauge F et al (2003) Treatment of pancreatic cancer: Challenge of the facts. World J Surg 27:1075–1084
5. Conroy T, Hammel P, Hebbar M et al (2018) FOLFIRINOX or Gemcitabine as Adjuvant Therapy for Pancreatic Cancer. N Engl J Med 379:2395–2406. https://doi.org/10.1056/NEJMoa1809775

6. Caravatta L, Macchia G, Mattiucci GC et al (2014) Inter-observer variability of clinical target volume delineation in radiotherapy treatment of pancreatic cancer: A multi-institutional contouring experience. Radiat Oncol 9:1–9. https://doi.org/10.1186/1748-717X-9-198

7. Mancuso A, Calabrò F, Sternberg CN (2006) Current therapies and advances in the treatment of pancreatic cancer. Crit Rev Oncol Hematol 58:231–241

8. Kayahara M, Nagakawa T, Ueno K et al (1993) An evaluation of radical resection for pancreatic cancer based on the mode of recurrence as determined by autopsy and diagnostic imaging. Cancer 72:2118–2123. https://doi.org/10.1002/1097-0142(19931001)72:7%3c2118::AID-CNCR2820720710%3e3.0.CO;2-4

9. Uhrich KE, Cannizzaro SM, Langer RS, Shakesheff KM (1999) Polymeric Systems for Controlled Drug Release. Chem Rev 99:3181–3198. https://doi.org/10.1021/cr940351u

10. Qi Y, Min H, Mujeeb A et al (2018) Injectable Hexapeptide Hydrogel for Localized Chemotherapy Prevents Breast Cancer Recurrence. ACS Appl Mater Interfaces 10:6972–6981. https://doi.org/10.1021/acsami.7b19258

11. Bu LL, Yan J, Wang Z et al (2019) Advances in drug delivery for post-surgical cancer treatment. Biomaterials 219:119182

12. Hadjianfar M, Semnani D, Varshosaz J (2018) Polycaprolactone/chitosan blend nanofibers loaded by 5-fluorouracil: An approach to anticancer drug delivery system. Polym Adv Technol 29:2972–2981. https://doi.org/10.1002/pat.4417

13. Labet M, Thielemans W (2009) Synthesis of polycaprolactone: A review. Chem Soc Rev 38:3484–3504. https://doi.org/10.1039/b820162p

14. Lavielle N, Popa AM, De Geus M et al (2013) Controlled formation of poly(ε-caprolactone) ultrathin electrospun nanofibers in a hydrolytic degradation-assisted process. Eur Polym J 49:1331–1336. https://doi.org/10.1016/j.eurpolymj.2013.02.038

15. Herrero-Herrero M, Gómez-Tejedor JA, Vallés-Lluch A (2018) PLA/PCL electrospun membranes of tailored fibres diameter as drug delivery systems. Eur Polym J 99:445–455. https://doi.org/10.1016/j.eurpolymj.2017.12.045

16. Iqbal S, Rashid MH, Arbab AS, Khan M (2017) Encapsulation of anticancer drugs (5-Fluorouracil and Paclitaxel) into polycaprolactone (PCL) nanofibers and in vitro testing for sustained and targeted therapy. J Biomed Nanotechnol 13:355–366. https://doi.org/10.1166/jbn.2017.2353

17. Torres-Martinez EJ, Cornejo Bravo JM, Serrano Medina A et al (2018) A Summary of Electrospun Nanofibers as Drug Delivery System: Drugs Loaded and Biopolymers Used as Matrices. Curr Drug Deliv 15:1360–1374. https://doi.org/10.2174/1567201815666180723114326

18. Rathbone MJ, Drummond BK, Tucker IG (1994) The oral cavity as a site for systemic drug delivery. Adv Drug Deliv Rev 13:1–22

19. Yang J, Wang S, Liu P et al (2017) Platelet-inspired medicine for tumor therapy Oncotarget 8:115748–115753

20. Tiwari G, Tiwari R, Bannerjee S et al (2012) Drug delivery systems: An updated review. Int J Pharm Investig 2:2. https://doi.org/10.4103/2230-973x.96920

21. Gong J, Chen M, Zheng Y et al (2012) Polymeric micelles drug delivery system in oncology. J Control Release 159:312–323

22. Rafei H, Mehta RS, Rezvani K (2019) Editorial: Cellular Therapies in Cancer. Front Immunol 10:2788

23. Prajapati SK, Jain A, Jain A, Jain S (2019) Biodegradable polymers and constructs: A novel approach in drug delivery. Eur Polym J 120:109191

24. Ranganath SH, Wang CH (2008) Biodegradable microfiber implants delivering paclitaxel for post-surgical chemotherapy against malignant glioma. Biomaterials 29:2996–3003. https://doi.org/10.1016/j.biomaterials.2008.04.002

25. Zhang J, Wang X, Liu T et al (2016) Antitumor activity of electrospun polylactide nanofibers loaded with 5-fluorouracil and oxaliplatin against colorectal cancer. Drug Deliv 23:794–800. https://doi.org/10.3109/10717544.2014.916768

26. Lee PI (1985) Kinetics of drug release from hydrogel matrices. J Control Release 2:277–288. https://doi.org/10.1016/0168-3659(85)90051-3

27. Subbiah T, Bhat GS, Tock RW et al (2005) Electrospinning of nanofibers. J Appl Polym Sci 96:557–569. https://doi.org/10.1002/app.21481

28. Deitzel J, Kleinmeyer J, Harris D, Beck TN (2001) The effect of processing variables on the morphology of electrospun nanofibers and textiles. Polymer (Guildf) 42:261–272. https://doi.org/10.1016/S0032-3861(00)00250-0

29. Athira KS, Sanpui P, Chatterjee K (2014) Fabrication of Poly(Caprolactone) Nanofibers by Electrospinning. J Polym Biopolym Phys Chem 2:62–66. https://doi.org/10.12691/jpbpc-2-4-1

30. Silke Megelski †, Jean S. Stephens †, D. Bruce Chase ‡ and, John F. Rabolt* † (2002) Micro- and Nanostructured Surface Morphology on Electrospun Polymer Fibers. https://doi.org/10.1021/MA020444A

31. Zong X, Kim K, Fang D et al (2002) Structure and process relationship of electrospun bioabsorbable nanofiber membranes. Polymer (Guildf) 43:4403–4412. https://doi.org/10.1016/S0032-3861(02)00275-6

32. Wang N, Zhao Y (2018) Coaxial electrospinning. Elsevier

33. Jiang H, Wang L, Zhu K (2014) Coaxial electrospinning for encapsulation and controlled release of fragile water-soluble bioactive agents. J Control Release 193:296–303. https://doi.org/10.1016/j.jconrel.2014.04.025

34. Qin X (2017) Coaxial electrospinning of nanofibers. Electrospun Nanofibers. https://doi.org/10.1016/B978-0-08-100907-9.00003-9

35. Faris JE, Blaszkowsky LS, McDermott S et al (2013) FOLFIRINOX in Locally Advanced Pancreatic Cancer: The Massachusetts General Hospital Cancer Center Experience. Oncologist 18:543–548. https://doi.org/10.1634/theoncologist.2012-0435

36. Conroy T, Gavoille C, Samalin E et al (2013) The role of the FOLFIRINOX regimen for advanced pancreatic cancer. Curr Oncol Rep 15:182–189. https://doi.org/10.1007/s11912-012-0290-4

37. Rustum YM (1990) Biochemical rationale for the 5-fluorouracil leucovorin combination and update of clinical experience. J Chemother 2(Suppl 1):5–11. https://doi.org/10.1080/1120009x.1990.11738998

38. Ivaturi VD, Kim SK (2009) Enhanced permeation of methotrexate in vitro by ion pair formation with L-arginine. J Pharm Sci 98:3633–3639. https://doi.org/10.1002/jps.21663

39. Chemocare 5-fluorouracil - Chemocare. http://chemocare.com/es/chemotherapy/drug-info/5-fluorouracil.aspx. Accessed 9 Apr 2021

40. Chemocare Metotrexato - Chemocare. http://chemocare.com/es/chemotherapy/drug-info/metotrexato.aspx. Accessed 9 Apr 2021

41. Tseng YY, Su CH, Yang ST, et al (2016) Advanced interstitial chemotherapy combined with targeted treatment of malignant glioma in rats by using drug-loaded nanofibrous membranes. Oncotarget 7:59902–59916. https://doi.org/10.18632/oncotarget.10989

42. Yohe ST, Herrera VLM, Colson YL, Grinstaff MW (2012) 3D superhydrophobic electrospun meshes as reinforcement materials for sustained local drug delivery against colorectal cancer cells. J Control Release 162:92–101. https://doi.org/10.1016/j.jconrel.2012.05.047

43. Singh M, Singh R, Dhami MK (2020) Biocompatible Thermoplastics as Implants/Scaffold. In: Reference Module in Materials Science and Materials Engineering. Elsevier

44. Mclauchlin AR, Thomas NL (2012) Biodegradable polymer nanocomposites. In: Advances in Polymer Nanocomposites: Types and Applications. Elsevier Inc., pp 398–430

45. Jiang L, Zhang J (2013) Biodegradable Polymers and Polymer Blends. In: Handbook of Biopolymers and Biodegradable Plastics: Properties, Processing and Applications. Elsevier Inc., pp 109–128

46. Xia G, Zhang H, Cheng R et al (2018) Localized Controlled Delivery of Gemcitabine via Microsol Electrospun Fibers to Prevent Pancreatic Cancer Recurrence. Adv Healthc Mater. https://doi.org/10.1002/adhm.201800593

Authors and Affiliations

Oihane Mitxelena-Iribarren[1,2] ⬤ **· Marc Riera-Pons**[1,2] **· Sheila Pereira**[3,4] **·**
Francisco José Calero-Castro[3,4] **· Juan Manuel Castillo Tuñón**[5] **·**
Javier Padillo-Ruiz[3,4,6] **· Maite Mujika**[1,2] **· Sergio Arana**[1,2]

[1]   CEIT-Basque Research and Technology Alliance (BRTA), Manuel Lardizábal 15,
     20018 Donostia-San Sebastián, Spain

[2]   Universidad de Navarra, Manuel Lardizábal 13, 20018 TecnunDonostia-San Sebastián, Spain

[3]   Department of General Surgery, Hospital University Virgen del Rocio, CSIC, IBiS, University
     of Seville, Seville, Spain

[4]   Oncology Surgery, Cell Therapy, and Organ Transplantation Group, Institute of Biomedicine
     of Seville (IBiS), Virgen del Rocio University Hospital, University of Seville, Seville, Spain

[5]   Department of Hepatobiliary and Pancreatic Surgery and Liver Transplantation, University
     Hospital of Badajoz, Badajoz, Spain

[6]   Surgery Department, University of Seville, Seville, Spain